Liquid Crystals
Publication details, including instructions for authors and subscription information:
http://www.informaworld.com/smpp/title~content=t713926090

Can <P_4> be obtained from fluorescence depolarization in nematics? Disc-like probes

A. Arcioni[a]; R. Tarroni[a]; C. Zannoni[a]
[a] Dipartimento di Chimica Fisica ed Inorganica, Universita, Bologna, Italy

To cite this Article Arcioni, A. , Tarroni, R. and Zannoni, C.(1989) 'Can <P_4> be obtained from fluorescence depolarization in nematics? Disc-like probes', Liquid Crystals, 6: 1, 63 — 74
To link to this Article: DOI: 10.1080/02678298908027323
URL: http://dx.doi.org/10.1080/02678298908027323

LIQUID CRYSTALS, 1989, VOL. 6, NO. 1, 63–74

Can $\langle P_4 \rangle$ be obtained from fluorescence depolarization in nematics? Disc-like probes

by A. ARCIONI, R. TARRONI and C. ZANNONI
Dipartimento di Chimica Fisica ed Inorganica, Universita', Viale Risorgimento, 4, 40136 Bologna, Italy

(*Received 21 November 1988; accepted 28 January 1989*)

The determination of the fourth rank orientational order parameter, $\langle P_4 \rangle$, is an important goal in liquid crystal research. Here we have looked at the feasibility of obtaining $\langle P_4 \rangle$ for a disc-like probe molecule from a time dependent fluorescence depolarization experiment. Simulated data at various temperatures have been prepared and then analyzed both individually and simultaneously using the global target deconvolution procedure. We have examined, in particular, the case of molecules subject to effective potentials containing a combination of second and fourth rank terms.

1. Introduction

Time dependent and to some extent steady state fluorescence polarization experiments can, in principle, provide not only second rank, but also fourth rank order parameters [1, 2]. However, the possibility of actually obtaining this kind of information from a real experiment is not to be taken for granted and will depend on a number of circumstances, partly of instrumental and partly of molecular origin [3, 4]. On the instrumental side of foremost importance is the need to deconvolute the time dependent intensities using a suitable instrument function. This is a well-studied subject that has received much attention in the past [5–8]. On the molecular side the shape and symmetry of the probe is significant, as is the orientation of the absorption and emission transition moments [3] μ and $\bar{\mu}$ in the molecular frame. Further what can be obtained from a certain experiment will depend on the relative time scales of the fluorescence decay and reorientation processes, τ_F and τ_R [1, 3]. Since the initial time anisotropy depends both on $\langle P_2 \rangle$ and $\langle P_4 \rangle$ we expect the fourth rank order parameter $\langle P_4 \rangle$ for the probe to be more accessible when the fluorescence decay time τ_F is so short that the initial decay is effectively sampled. In this case it is also important that $\langle P_2 \rangle$ can be determined as well. In the opposite limit, when fluorescence decay is much slower than reorientation the photoselected molecules have time to relax to orientational equilibrium and only the second rank Legendre polynomial average $\langle P_2 \rangle$ can be obtained reliably. The maximum amount of information can be extracted from experiments when the time evolution of fluorescence depolarization is followed [9, 10]. For a probe with arbitrary orientation of the absorption and emission transition moments various linear combinations of orientational correlation functions contribute to the observable intensities. For a planar disc-like probe with transition moments perpendicular to the molecule symmetry axis we shall see later that at least two correlation functions contribute to the intensities. One refers to disc axis reorientation with respect to the director (tumbling). The other refers to molecular spinning around the disc axis. Experimental and data analysis problems make the

0267–8292/89 $3.00

situation more complex. The determination of molecular parameters with a single photon counting apparatus normally requires a delicate deconvolution procedure [5, 7]. Even with faster response apparatus [9] accessing the initial part of the decay is troublesome. We have treated the case of rod-like probes elsewhere [4]. There we have found that the second rank order parameter $\langle P_2 \rangle$ can be obtained relatively easily. On the other hand, obtaining the fourth rank order parameter $\langle P_4 \rangle$ is facilitated by simultaneously deconvoluting data at various temperatures, using the deconvolution procedure that we have called global target analysis [10]. In the present paper we investigate to what extent molecular information can actually be extracted from experimental data on disc-like probes. There are various fluorescent probes that belong to this class [2, 11]. Some, like coronene [2, 12] and triphenylene [2, 12] have high enough symmetry to be considered discs for our purposes. Other frequently employed reporter molecules and particularly condensed hydrocarbons like perylene [12–15] and pyrene [16] have approximate disc shapes, although they do strictly behave as biaxial objects [17, 18]. As in [4] we shall construct sets of simulated data representative of a few important experimental conditions and analyse them with various procedures. As we shall see the present class of molecules is sufficiently different from those treated previously to warrant a separate discussion.

2. Fluorescence depolarization theory

Here we recall the essentials of the theory of fluorescence depolarization in liquid crystals which has been described in detail elsewhere [1, 10] in order to establish the notation and to prepare the ground for the data analysis section. We assume the laboratory Z axis parallel to the preferred orientation (director) of a uniformly aligned liquid crystal sample placed at the origin of the coordinate system. The exciting light beam is plane polarized with polarization direction $\mathbf{e}_i$ and is approaching along the laboratory Y axis. The fluorescent probe has effective disc-like symmetry, i.e. we assume that its ordering matrix cannot be distinguished from a genuinely cylindrical one. The absorption and emission transition moments μ and $\bar{\mu}$ lie in the disc plane, perpendicular to the effective symmetry axis. The dye concentration is assumed to be so low that probe–probe intermolecular relaxation effects can be neglected and the pulse intensity to be weak enough to avoid saturation effects [19]. Fluorescence light is observed in the forward or alternatively in the orthogonal direction through an analyser, set at a direction of polarization $\mathbf{e}_f$. Typically the excitation polarizer is kept along Z while the appropriate fluorescence intensities at a time t after an instantaneous excitation pulse can be written, when reorientation is the dominant depolarization mechanism and the fluorescence and reorientation processes are statistically independent, as

$$I_{ZZ}(t) = F(t)\,[\tfrac{1}{9} + \tfrac{1}{3}(\tfrac{2}{3})^{1/2}\langle P_2\rangle\,(\bar{A}^{2,0}_{\mathrm{MOL}} + A^{2,0}_{\mathrm{MOL}}) + \tfrac{2}{3}G_0(t)], \tag{1}$$

$$I_{ZX}(t) = F(t)\,[\tfrac{1}{9} + \tfrac{1}{6}(\tfrac{2}{3})^{1/2}\langle P_2\rangle\,(2\bar{A}^{2,0}_{\mathrm{MOL}} - A^{2,0}_{\mathrm{MOL}}) - \tfrac{1}{3}G_0(t)], \tag{2}$$

where $A^{2,m}_{\mathrm{MOL}}$, $\bar{A}^{2,m}_{\mathrm{MOL}}$ are spherical components of the absorption and emission tensors $\mathbf{A} = \boldsymbol{\mu} \times \boldsymbol{\mu}$ and $\bar{\mathbf{A}} = \bar{\boldsymbol{\mu}} \times \bar{\boldsymbol{\mu}}$, direct products of the transition moments $\boldsymbol{\mu}$ and $\bar{\boldsymbol{\mu}}$. $F(t)$ is a fluorescence decay function and

$$G_q(t) = \sum_n A^{2,n}_{\mathrm{MOL}}\bar{A}^{2,n^*}_{\mathrm{MOL}}\phi_{qn}(t) \tag{3}$$

is a linear combination of second rank orientational correlation functions $\phi_{qn}(t)$ [20]

$$\phi_{qn}(t) = \langle D^2_{qn}(\omega_0)D^{2^*}_{qn}(\omega_t)\rangle. \tag{4}$$

Here $D^L_{ab}(\alpha\beta\gamma)$ is a Wigner rotation matrix [21] and the angular brackets indicate an average over the molecular orientations ω_0 and ω_t at time zero and at time t. These orientational auto-correlation functions describe the rotational dynamics of the probe. We also introduce the theoretical fluorescence anisotropy ratio

$$r(t) = \frac{I_{ZZ}(t) - I_{ZX}(t)}{I_{ZZ}(t) + 2I_{ZX}(t)}. \tag{5}$$

We examine here two configurations corresponding to transition moments in the disc plane. First we consider a probe with absorption and emission transition moments parallel to the molecular x axis, so that the appropriate transition tensor components are

$$A^{2,0}_{\mathrm{MOL}} = \bar{A}^{2,0}_{\mathrm{MOL}} = -\sqrt{\tfrac{1}{6}}, \tag{6a}$$

$$A^{2,\pm 2}_{\mathrm{MOL}} = \bar{A}^{2,\pm 2}_{\mathrm{MOL}} = \tfrac{1}{2}. \tag{6b}$$

In this case the intensities are

$$I_{ZZ}(t) = F(t)\,[\tfrac{1}{9} - \tfrac{2}{9}\langle P_2 \rangle + \tfrac{1}{9}\phi_{00}(t) + \tfrac{1}{3}\phi_{02}(t)] \tag{7}$$

and

$$I_{ZX}(t) = F(t)\,[\tfrac{1}{9} - \tfrac{1}{18}\langle P_2 \rangle - \tfrac{1}{18}\phi_{00}(t) - \tfrac{1}{6}\phi_{02}(t)]. \tag{8}$$

We also have the theoretical anisotropy

$$r(t) = \frac{\langle P_2 \rangle - 3\phi_{02} - \phi_{00}}{2\langle P_2 \rangle - 2}, \tag{9}$$

with the value

$$r(0) = \frac{27\langle P_4 \rangle - 55\langle P_2 \rangle + 28}{70 - 70\langle P_2 \rangle}, \tag{10}$$

at time zero and at time going to infinity

$$r(\infty) = -\tfrac{1}{2}\langle P_2 \rangle. \tag{11}$$

The other configuration we have studied is one with perpendicular absorption and emission moments: $\boldsymbol{\mu} \parallel \mathbf{y}$, $\bar{\boldsymbol{\mu}} \parallel \mathbf{x}$, corresponding to

$$A^{2,0}_{\mathrm{MOL}} = \bar{A}^{2,0}_{\mathrm{MOL}} = -\sqrt{\tfrac{1}{6}}, \tag{12a}$$

$$A^{2,\pm 2}_{\mathrm{MOL}} = -\bar{A}^{2,\pm 2}_{\mathrm{MOL}} = -\tfrac{1}{2}. \tag{12b}$$

This gives

$$I_{ZZ}(t) = F(t)\,[\tfrac{1}{9} - \tfrac{2}{9}\langle P_2 \rangle + \tfrac{1}{9}\phi_{00}(t) - \tfrac{1}{3}\phi_{02}(t)] \tag{13}$$

$$I_{ZX}(t) = F(t)\,[\tfrac{1}{9} - \tfrac{1}{18}\langle P_2 \rangle - \tfrac{1}{18}\phi_{00}(t) + \tfrac{1}{6}\phi_{02}(t)] \tag{14}$$

and the anisotropy ratio

$$r(t) = \frac{\langle P_2 \rangle + 3\phi_{02} - \phi_{00}}{2\langle P_2 \rangle - 2}. \tag{15}$$

The limiting values at short and long times are

$$r(0) = \frac{9\langle P_4 \rangle + 5\langle P_2 \rangle - 14}{70 - 70\langle P_2 \rangle} \tag{16}$$

$$r(\infty) = -\tfrac{1}{2}\langle P_2 \rangle. \tag{17}$$

The order parameters that can be obtained for a probe with effective cylindrical symmetry are at the most $\langle P_2 \rangle$ and $\langle P_4 \rangle$. Thus the least biased singlet orientational distribution $f(\beta)$ we can infer from a depolarization experiment utilizing maximum entropy principles [22, 23] is

$$f(\beta) = \exp [a_0 + a_2 P_2 (\cos \beta) + a_4 P_4 (\cos \beta)], \tag{18}$$

where a_0 is determined from the normalization condition of $f(\beta)$ and a_2, a_4 are temperature dependent quantities that should reproduce the experimental $\langle P_2 \rangle$ and $\langle P_4 \rangle$. In practice what is actually observed is a set of intensities and we shall try to fit them to a theoretical model based on the distribution in equation (18). In particular the computation of theoretical intensities is accomplished assuming that the reorientation of the molecules in the anisotropic potential

$$-U_{\text{probe}}(\beta)/kT = a_2 P_2 (\cos \beta) + a_4 P_4 (\cos \beta) \tag{19}$$

is diffusional. A rotation equation of motion can then be set up in the usual way [24] and orientational auto-correlation functions can be calculated in terms of the potential in equation (19). No additional approximation is needed, although sometimes [25–27] a strongly simplified analytical form of the orientational auto-correlation functions is employed. This approximation, although convenient, is not always successful [3, 4] and so in the remainder of this paper we shall always use the full numerical solution.

3. Preparation of temperature dependent simulated data

We have shown elsewhere [3] that a useful way of analysing temperature dependent anisotropy data is to perform simultaneous deconvolution of the intensities in terms of the target static and dynamic molecular parameters. We have called this approach, described in detail in [10] a global target analysis. Since our purpose here is to test the accessibility of the desired microscopic information, the first step is to prepare a realistic set of simulated intensities at a number of temperatures. To do this we prepare theoretical intensity curves using equations (1) and (2) we have seen earlier on and an assumed instrument function [6]. Then Poisson noise to a predetermined level is added. The data obtained in this way are treated as true experimental data and analysed to see if the molecular parameters can be recovered for those simulated conditions. We have assumed that the probe experiences rotational diffusion in an effective potential of the kind given by the Humphries–James–Luckhurst molecular field theory for second and fourth rank interactions between solute and solvent [28, 29]. This $P_2 - P_4$ potential is

$$-U_{\text{probe}}(\beta) = u_2 \langle P_2 \rangle_{\text{solv}} P_2 (\cos \beta) + u_4 \langle P_4 \rangle_{\text{solv}} P_4 (\cos \beta), \tag{20}$$

where u_2, u_4 are solute-solvent interaction coefficients and $\langle P_L \rangle_{\text{solv}}$ are pure solvent order parameters. The pure solvent order parameters are in turn obtained assuming that a Humphries–James–Luckhurst [28] molecular field applies to the pure nematic, i.e.

$$-U_{\text{solv}}(\beta) = c_2 [\langle P_2 \rangle_{\text{solv}} P_2 (\cos \beta) + \lambda_{\text{solv}} \langle P_4 \rangle_{\text{solv}} P_4 (\cos \beta)], \tag{21}$$

where c_2 is a solvent–solvent interaction energy and λ_{solv} is the ratio between the fourth rank and second rank interaction coefficients. The solvent order parameters $\langle P_2 \rangle_{\text{solv}}$ and $\langle P_4 \rangle_{\text{solv}}$ obey self consistency equations and are derived from molecular field

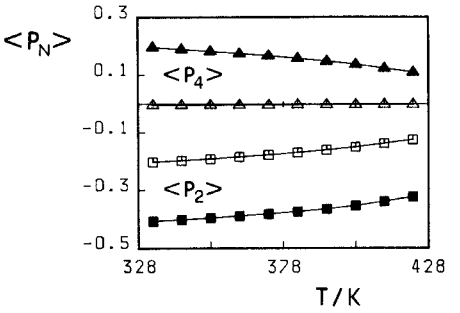

Figure 1. The second and fourth rank probe order parameters $\langle P_2 \rangle$ (squares), $\langle P_4 \rangle$ (triangles) for the two pseudo-experimental situations which we have simulated. The first (empty symbols) corresponds to $u_2/k = u_4/k = -800\,\mathrm{K}$, $\lambda_{\mathrm{solv}} = -0{\cdot}3$. The second (full symbols) to $u_2/k = -1800\,\mathrm{K}$, $u_4/k = 400\,\mathrm{K}$, $\lambda_{\mathrm{solv}} = 0{\cdot}3$. The temperature T ranges from 333 K to the nematic–isotropic value of 423 K. The continuous lines help to see the full temperature dependence.

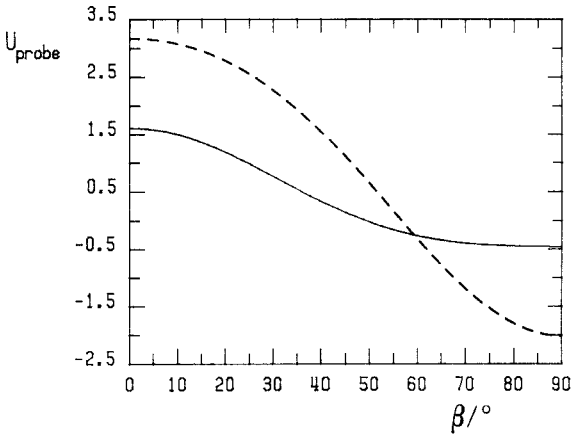

Figure 2. The effective probe potential $U_{\mathrm{probe}}(\beta)$ at $T = 373\,\mathrm{K}$ for two simulations belonging to family (I) $a_2 = -1{\cdot}2099$, $a_4 = -0{\cdot}3988$ (continuous line) and (II) $a_2 = -3{\cdot}6621$, $a_4 = 0{\cdot}4932$ (dashed line).

theory. They are defined at a certain temperature T when a nematic–isotropic transition temperature T_{NI} is assigned. As a special case the Maier–Saupe solvent potential would be obtained by letting $\lambda_{\mathrm{solv}} = 0$. Here we have chosen the coefficients in the potential to represent two quite different situations with order parameters pictured in figure 1. (I) The first case corresponds to a poorly oriented solute, with $\langle P_4 \rangle$ always near to zero (empty symbols in figure 1). To construct it we have used $u_2/k = u_4/k = -800\,\mathrm{K}$, $\lambda_{\mathrm{solv}} = -0.3$. (II) The second effective probe potential has a better ordering and $\langle P_4 \rangle$ is in any case clearly positive. The coefficients employed are $u_2/k = -1800\,\mathrm{K}$, $u_4/k = 400\,\mathrm{K}$, $\lambda_{\mathrm{solv}} = 0.3$. In any case the correspondence with a real temperature is obtained by fixing the nematic–isotropic transition temperature at $T = 423\,\mathrm{K}$. In figure 2 we show the two potentials at $T = 373\,\mathrm{K}$.

The main dynamic parameter is the perpendicular component of the diffusion tensor $D_\perp$ at the various temperatures. This has been assumed to follow an Arrhenius

type behaviour [10]

$$D_\perp(T) = D_\perp^0 \exp(-E_a/RT), \tag{22}$$

where E_a is an activation energy. In contrast the ratio $\eta = D_\parallel/D_\perp$ has been kept fixed. This implies the same activation energy for tumbling and spinning so it is probably not going to be very realistic but we shall assume it anyway for simplicity. A number of simulations and analyses have been performed and are reported in the next section. In all the cases treated we have used $D_\perp^0 = 400\,\text{ns}^{-1}$, $E_a = 29{\cdot}3\,\text{kJ/mol}$. We have convoluted the theoretical intensities I_{ij} with the instrumental function as described in [3, 7]. The pulse function employed is [6, 7]

$$P(t) = at^3 \exp(-t), \tag{23}$$

with a determining the count level. In our simulations we take $a = 5 \times 10^4$, which yields typical count levels for $I_\parallel + 2I_\perp$ between 60 kcounts and 80 kcounts at peak level, a range of values accessible with a single photon apparatus. We consider intensity histograms over 256 channels with a width of 0·08 ns. We also include scattered light, as a fraction of the pulse, on the parallel (10 per cent) and on the perpendicular channel (1 per cent) and a time shift of 0·1 ns. The fluorescence of the probe is assumed to decay exponentially, with a fluorescence time $\tau_F = 5\,\text{ns}$.

4. Data analysis

We have employed three different strategies.

4.1. *Individual target analysis for each temperature*

This is the most straightforward procedure. It consists of analysing each temperature on its own. We call target analysis the procedure of doing deconvolution not to a sum of free exponentials but rather to the parameters in the model employed (here the diffusional one) [7]. Target analysis is performed on each set of data to determine in particular $a_2(T)$, $a_4(T)$ in equation (19) together with $D_\perp(T)$. We also employ the results of this analysis as a guideline for starting the global procedure described in what follows.

4.2. *Humphries–James–Luckhurst globalization*

This is a global fit to the Humphries–James–Luckhurst (HJL) parameters u_2/k, u_4/k, λ_{solv} in equation (20) and (21). We have also performed a diffusion tensor globalization by assuming an Arrhenius type law for the component of the probe rotational diffusion tensor **D** perpendicular to the long axis, as in [10]. Thus, we also fit $D_\perp^0$, E_a and η. In principle this analysis is just a check rather than anything else, since we have constructed the data using these very equations, so that we should have $a_2(T) = u_2\langle P_2\rangle_{\text{solv}}/kT$, $a_4(T) = u_4\langle P_4\rangle_{\text{solv}}/kT$. In practice, however, it is an important test of the feasibility of the complex non-linear fit problem we have set up.

4.3. *Parabolic global target analysis*

A severe limitation of global analysis would seem that in many practical situations a reasonable theoretical expression for fitting the relative fourth rank and second rank contributions will not be known. Thus the only alternative would appear to be to perform individual analysis or at most a diffusion tensor globalization. However, we

believe we still possess some useful information on the temperature dependence of a_2, a_4 in equation (18) or alternatively of the probe order parameters $\langle P_2 \rangle$ and $\langle P_4 \rangle$. In particular we expect that their values fall on a continuous and differentiable curve, and possibly a smooth one as long as the various temperatures belong to the same (nematic or isotropic) phase. It is clear that the detailed form of this dependence is unknown, but we should also realize that analyzing the experimental intensities for various temperatures independently would not implement the simple but important continuity constraints we have just mentioned. A possible approach is then to assume an empirical form for $a_2(T)$, $a_4(T)$ or both, which is flexible enough to accommodate every realistic variation that can take place in the data. Since $\langle P_2 \rangle$ and thus indirectly a_2 is normally well determined, we have chosen to globalize just $a_4(T)$. The simplest choice is to take a polynomial or truncated Taylor expansion starting from the lowest temperature $T_{\min}$. Thus, we have assumed a simple quadratic dependence for the temperature variation of a_4

$$a_4(T) = \lambda_0 + \lambda_1 (T - T_{\min}) + \lambda_2 (T - T_{\min})^2, \tag{24}$$

where λ_0, λ_1, λ_2 are to be determined globally. Notice that no particular physical significance is attached at the moment to the coefficients. Indeed other analytical forms could be used in place of equation (24). We emphasize that the objective is to introduce the requisite of smoothness of the order parameters as a function of temperature as a means of associating measurements at different temperatures. In this approach the parameter $a_2(T)$ is determined individually, while $D_\perp(T)$ and η are globalized as in the previous section.

5. Results

We shall examine results for potential I and II in turn.

5.1. *Potential I*

We have studied data for ten temperatures regularly spaced between $T = 333\,\mathrm{K}$ and 423 K. The theoretical anisotropies $r(t)$ are shown in figure 3 for these two

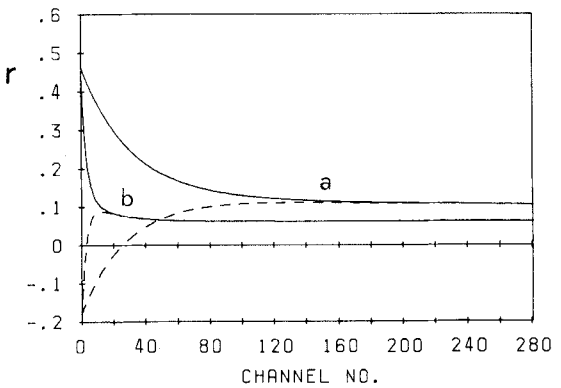

Figure 3. Theoretical anisotropies $r(t)$ for an oblate probe in the effective potential I. The continuous lines correspond to $\boldsymbol{\mu} \parallel \bar{\boldsymbol{\mu}} \parallel \mathbf{x}$ (cf. equation (9)). The dashed lines correspond to $\boldsymbol{\mu} \parallel \mathbf{y}$, $\bar{\boldsymbol{\mu}} \parallel \mathbf{x}$ (cf. equation (15)). We show curves at $T = 333\,\mathrm{K}$ (*a*) and at 423 K (*b*), i.e. at the lowest and highest temperatures studied.

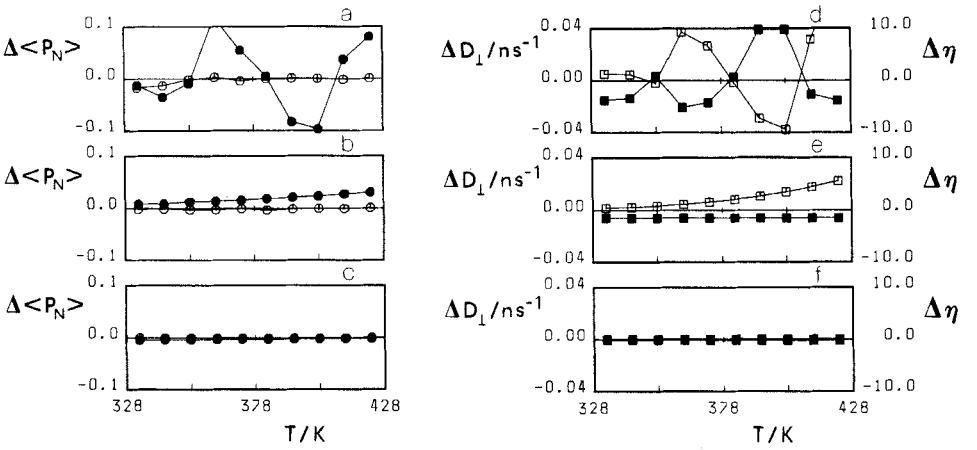

Figure 4. Results of a $P_2 - P_4$ analysis of the fluorescence intensities corresponding to a disc-like probe with $\boldsymbol{\mu} \parallel \tilde{\boldsymbol{\mu}} \parallel \mathbf{x}$. The symbols correspond to the difference Δ between recovered and exact results for $\langle P_2 \rangle$ (empty circles), $\langle P_4 \rangle$ (full circles), for $D_\perp$ (empty squares) and for η (full squares) when analysing with individual target analysis (*a*), (*d*), parabolic global target analysis (*b*), (*e*) and with HJL global target analysis (*c*), (*f*). The continuous lines are just a guide to the eye.

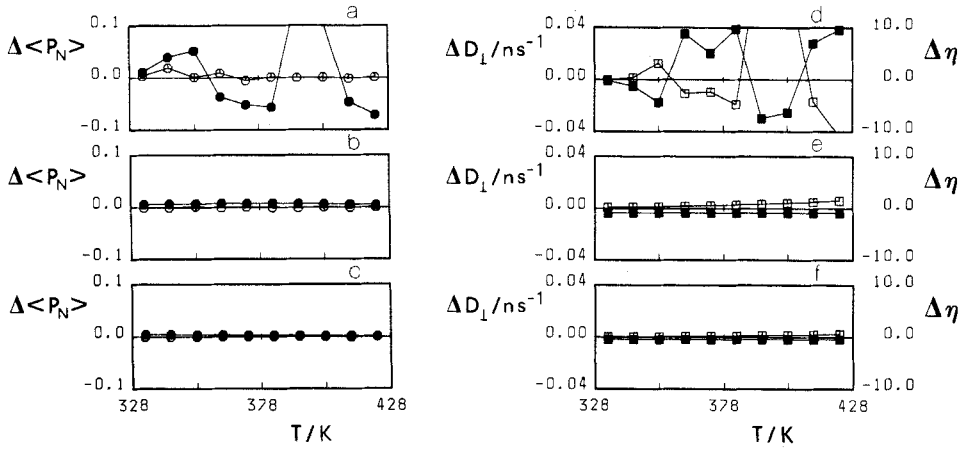

Figure 5. Results of a $P_2 - P_4$ analysis of the fluorescence intensities corresponding to a disc-like probe with $\boldsymbol{\mu} \parallel \mathbf{y}$, $\tilde{\boldsymbol{\mu}} \parallel \mathbf{x}$. The symbols correspond to the difference Δ between recovered and exact results for $\langle P_2 \rangle$ (empty circles), $\langle P_4 \rangle$ (full circles), for $D_\perp$ (empty squares) and for η (full squares) when analysing with individual target analysis (*a*), (*d*), parabolic global target analysis (*b*), (*e*) and with HJL global target analysis (*c*), (*f*). The continuous lines are just a guide to the eye.

extreme temperatures and for the two transition moment configurations described previously. We notice that the polarization anisotropy starts from a positive or negative value respectively for a parallel (cf. equation (10)) or perpendicular (cf. equation (16)) configuration of in-plane transition moments. However both curves then become positive and indeed converge to the same plateau value (cf. equation (11) and (17)).

The results of our analyses are shown in figures 4 and 5 for the parallel and perpendicular transition moment configurations. We have chosen to present the

deviations between the true input values and those recovered for the various techniques to make immediately apparent the performance of the different data analysis methods. In figures 4, 5 we show the differences $\Delta\langle P_2 \rangle$, $\Delta\langle P_4 \rangle$, $\Delta D_\perp$, $\Delta\eta$ between the recovered and exact results for the second and fourth rank order parameters and, respectively, for the dynamic quantities. In (*a*), (*d*) we present the differences resulting by analysing each temperature independently. As we can see the only quantity well recovered with this straightforward individual target analysis is the second rank order parameter. We observe in particular strong correlations between $\langle P_4 \rangle$, $D_\perp(T)$ and η which make the values obtained for these quantities hardly meaningful.

It is important to notice that the information on these quantities is not out of reach. Indeed performing a simple parabolic global target analysis, yields for the static and dynamic observables the values reported in plates (*b*), (*e*) of the same figures. In this case the results are greatly improved over the previous kind of analysis. The global fit to the Humphries–James–Luckhurst parameters shown in (*c*), (*f*) again of the same figures shows that perfect agreement could be reached, i.e. that the non-linear inverse problem we are attacking is soluble if the correct equation linking data at different temperatures can be guessed.

5.2. *Potential II*

This second model potential corresponds (cf. figure 1) to a more markedly ordered probe ($\langle P_2 \rangle$ is much nearer than before to its complete order limit of $-1/2$). At the same time $\langle P_4 \rangle$ is large and positive. The calculated anisotropies are plotted in figure 6 for the lowest and highest temperature studied and for the two transition moment geometries.

We now report in figures 7 and 8 the results of the various analyses performed for the parallel and perpendicular transition moment configuration. We employ, of course, the same notation as before. The first thing to notice is that in this case the analyses are generally poorer than for the previous potential. This must be partly due to an increase in difficulty due to the present parameters combination. Indeed the HJL global analysis itself, which is our internal test, has some difficulty in recuperating the

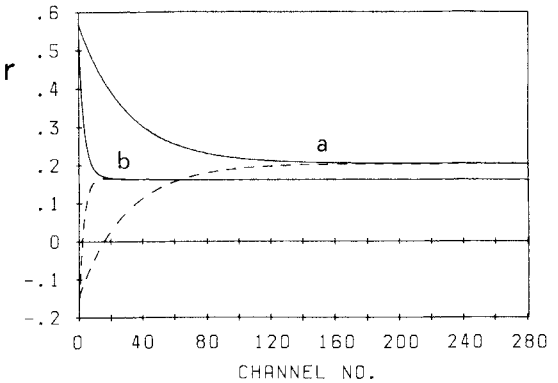

Figure 6. Theoretical anisotropies $r(t)$ for a disc-like probe subject to the effective potential II. The continuous lines corresponds to $\boldsymbol{\mu} \parallel \tilde{\boldsymbol{\mu}} \parallel \mathbf{x}$ (cf. equation (9)). The dashed lines correspond to $\boldsymbol{\mu} \parallel \mathbf{y}$, $\tilde{\boldsymbol{\mu}} \parallel \mathbf{x}$ (cf. equation (15)). We show curves at $T = 333$ K (*a*) and at 423 K (*b*), i.e. at the lowest and highest temperatures studied.

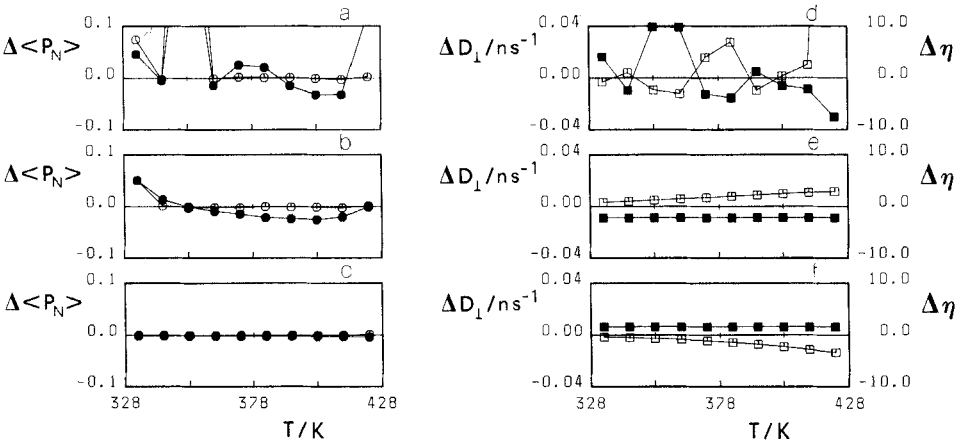

Figure 7. Analyses of the fluorescence intensities corresponding to the probe with $\mu \parallel \bar{\mu} \parallel x$ subject to potential II. The notation for the symbols is the same as in figure 4.

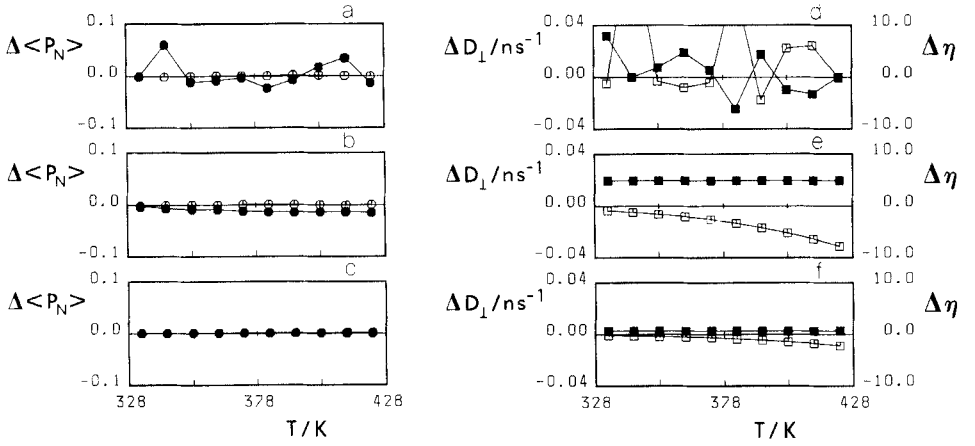

Figure 8. Results of the analysis for the probe in potential II and transition moments perpendicular to one another; the notation for the symbols is the same as in figure 5.

dynamic quantities, although both $\langle P_2 \rangle$ and $\langle P_4 \rangle$ are obtained very precisely. Given this increased difficulty it is not surprising that both the individual target analysis and the parabolic global target analysis work less satisfactorily than in the previous case. In figure 7 (*a*) we see that an individual analysis can occasionally give not only mediocre $\langle P_4 \rangle$, but even poor $\langle P_2 \rangle$. In one case both the order parameters were quite incorrect, with $\langle P_2 \rangle$ even of the wrong sign: at $T = 353$ K, $\langle P_2 \rangle = 0{\cdot}240$, $\langle P_4 \rangle = 0{\cdot}545$ were obtained instead of $\langle P_2 \rangle = -0{\cdot}3955$, $\langle P_4 \rangle = 0{\cdot}1832$. Notice that it would have been difficult to spot right away this incorrect result just on the basis of the quality of the fit. The reduced chi square χ_r^2 was in fact 1·061 for this individual analysis. Similar considerations apply to the diffusion tensor components (*d*).

The use of parabolic global target analysis sensibly improves the situation as we see from figures 8 (*b*), (*e*).

6. Conclusions

We have shown that the order parameter $\langle P_2 \rangle$ and $\langle P_4 \rangle$ of a disc-like fluorescence probe can be obtained from time dependent polarization intensities if a suitable data analysis procedure is employed. This is particularly important for this kind of probe where the analysis proves more difficult than that for rod-like dyes. We believe the requirement of smoothness imposed on the order parameters to be particularly important to allow the data analysis procedure a selection of the proper solution amongst various statistically equivalent ones. For example Levine and coworkers [30] have observed that in their analysis of the rod-like probe 1,6 diphenyl hexatriene (DPH) and trimethyl ammonium-DPH (TMA-DPH) in POPC vesicles, equally good fits could be obtained with two rather different sets of molecular parameters. In that case the situation is worsened by the macroscopic isotropic symmetry which causes [20] the sign of $\langle P_2 \rangle$ to be undetermined from the plateau, but the problem stems again from having different statistically equivalent solutions. In any case the intercommunication between fits at different temperatures seems an important way of improving the physical significance of the data obtained.

We are grateful to Min. P.I. and C.N.R. for support toward the maintenance costs of the DEC VAX11-780 and VS2000 minicomputers as well as the FPS-164 array processor used in this work.

References

[1] ZANNONI, C., 1979, *Molec. Phys.*, **38**, 1813.
[2] MICHL, J., and THULSTRUP, E. W., 1987, *Spectroscopy with Polarized Light* (VCH).
[3] ARCIONI, A., TARRONI, R., and ZANNONI, C., 1988, *Polarized Spectroscopy of Ordered Systems*, edited by B. Samori' and E. Thulstrup (Kluwer), p. 421.
[4] ARCIONI, A., TARRONI, R., and ZANNONI, C., 1988, *Nuovo Cim.* D, **10**, 1409.
[5] CUNDALL, R. B., and DALE, R. E. (editors), 1983, *Time Resolved Fluorescence Spectroscopy in Biochemistry and Biology* (Plenum).
[6] MCKINNON, A., SZABO, A. G., and MILLER, D. R., 1977, *J. phys. Chem.*, **81**, 1564.
[7] ARCIONI, A., and ZANNONI, C., 1984, *Chem. Phys.*, **88**, 113.
[8] VAN DEN ZEGEL, M., BOENS, N., DAEMS, D., and DE SCHRYVER, F. C., 1986, *Chem. Phys.*, **101**, 311.
[9] GORDEEV, E. V., DOLGANOV, V. K., and KORSHUNOV, V. V., 1986, *Soviet Phys. JETP Lett.*, **43**, 766.
[10] ARCIONI, A., BERTINELLI, F., TARRONI, R., and ZANNONI, C., 1987, *Molec. Phys.*, **61**, 1161.
[11] BERLMAN, I. B., 1971, *Handbook of Fluorescence Spectra of Aromatic Molecules* (Academic Press).
[12] SACKMANN, E., KREBS, P., REGA, H. U., VOSS, J., and MÖHWALD, H., 1973, *Molec. Crystals liq. Crystals*, **24**, 283.
[13] BRAND, L., KNUTSON, J. R., DAVENPORT, L., BEECHEM, J. M., DALE, R. E., WALBRIDGE, D. G., and KOWALCZYK, A. A., 1985, *Spectroscopy and the Dynamics of Molecular Biological Systems*, edited by P. M. Bayley and R. E. Dale (Academic Press), p. 259.
[14] BARKLEY, M. D., KOWALCZYK, A. A., and BRAND, L., 1981, *J. chem. Phys.*, **75**, 3581.
[15] JOHANSSON, L. B.-Å., *Chem. Phys. Lett.*, **118**, 516.
[16] JOHANSSON, L. B.-Å., and LINDBLOM, G., 1986, *Liq. Crystals*, **1**, 53.
[17] MICHL, J., THULSTRUP, E. W., and EGGERS, J. H., 1970, *J. phys. Chem.*, **74**, 3878.
[18] SHILSTONE, G. N., ZANNONI, C., and VERACINI, C. A., *Liq. Crystals* (in the press).
[19] RAZI-NAQVI, K., 1980, *J. chem. Phys.*, **73**, 3019.
[20] ZANNONI, C., ARCIONI, A., and CAVATORTA, P., 1983, *Chem. Phys. Lipids*, **32**, 179.
[21] ROSE, M. E., 1957, *Elementary Theory of Angular Momentum* (Wiley).
[22] LEVINE, R. D., and TRIBUS, M. (editors), 1979, *The Maximum Entropy Formalism* (MIT Press).

[23] KOOYMAN, R. P. H., LEVINE, Y. K., and VAN DER MEER, B. W., 1981, *Chem. Phys.*, **60**, 317.
[24] NORDIO, P. L., and SEGRE, U., 1979, *The Molecular Physics of Liquid Crystals*, edited by G. R. Luckhurst and G. W. Gray (Academic Press), p. 411.
[25] AMELOOT, M., HENDRICKX, H., HERREMAN, W., POTTEL, H., VAN CAUWELAERT, F., and VAN DER MEER, B. W., 1984, *Biophys. J.*, **46**, 525.
[26] VAN DER MEER, B. W., POTTEL, H., HERREMAN, W., AMELOOT, M., HENDRICKX, H., and SCHRÖDER, H., 1984, *Biophys. J.*, **46**, 515.
[27] BEST, L., JOHN, E., and JÄHNIG, F., 1987, *Eur. J. Biophys.*, **15**, 87.
[28] HUMPHRIES, R. L., JAMES, P. G., and LUCKHURST, G. R., 1972, *J. chem. Soc. Faraday II*, **68**, 1031.
[29] LUCKHURST, G. R., and SETAKA, M., 1973, *Molec. Crystals liq. Crystals*, **19**, 279.
[30] VAN LANGEN, H., LEVINE, Y. K., AMELOOT, M., and POTTEL, H., 1987, *Chem. Phys. Lett.*, **140**, 394.